AGU ADVANCING EARTH AND SPACE SCIENCES

Geophysical Research Letters®

RESEARCH LETTER
10.1029/2025GL119267

Bridging the Gap Between the Earth's Ionosphere and Plasmasphere

Artem Smirnov[1,2], Yuri Shprits[2,3,4], Hermann Lühr[2], Elena A. Kronberg[1], Jerry Goldstein[5], Yoshizumi Miyoshi[6], Fabricio Prol[7,8], Alessio Pignalberi[9], Natalia Buzulukova[10,11], Nicholas Pedatella[12,13], Bernhard Haas[2], Dedong Wang[2], Yoshiya Kasahara[14], Fuminori Tsuchiya[15], Shoya Matsuda[14], Atsuki Shinbori[6], and Ayako Matsuoka[16]

[1]Department of Earth and Environmental Sciences, Ludwig Maximilian University of Munich, Munich, Germany, [2]GFZ Helmholtz Centre for Geosciences, Potsdam, Germany, [3]Institute of Physics and Astronomy, University of Potsdam, Potsdam, Germany, [4]Department of Earth, Planetary and Space Sciences, University of California Los Angeles, Los Angeles, CA, USA, [5]Southwest Research Institute, San Antonio, TX, USA, [6]Nagoya University, Nagoya, Japan, [7]Finnish Geospatial Research Institute (FGI), National Land Survey of Finland (NLS), Espoo, Finland, [8]School of Technology and Innovation, University of Vaasa, Vaasa, Finland, [9]National Institute of Geophysics and Volcanology (INGV), Rome, Italy, [10]NASA Goddard Space Flight Center, Greenbelt, MD, USA, [11]Department of Astronomy, University of Maryland, College Park, MD, USA, [12]High Altitude Observatory, National Center for Atmospheric Research, Boulder, CO, USA, [13]COSMIC Program Office, University Center for Atmospheric Research, Boulder, CO, USA, [14]Kanazawa University, Kanazawa, Japan, [15]Tohoku University, Uji, Japan, [16]Kyoto University, Sendai, Japan

Abstract Cold plasma distribution in the ionosphere-plasmasphere system governs wave-particle interactions, plasma energization and loss, and radio wave propagation. A longstanding observational gap at altitudes ~800–8,000 km has largely prevented studying the coupled dynamics of the two regions. Here, we show that observations by JAXA's Arase mission can bridge this gap. Electron densities inferred from the upper hybrid resonance frequencies measured by Arase are highly consistent with radio occultation profiles from the Constellation Observing System for Meteorology, Ionosphere and Climate (COSMIC) mission, with a median difference of ~5%. Using the combined COSMIC-Arase data set, we provide a convenient way to reconcile the two regions in empirical models based on the analytical Chapman function inversion for scale height. Our results enable studying fundamental questions about the ionosphere-plasmasphere coupling, their transition, and life cycle of cold plasma in near-Earth space.

Plain Language Summary Cold plasma in the ionosphere and plasmasphere plays a critical role in the dynamics of near-Earth space environment. The physical processes within these two regions are different but tightly coupled. Ionospheric particles fill the plasmasphere on the dayside, while the plasmaspheric particles descend into the ionosphere at night and help sustain it in the absence of photoionization. However, how exactly these populations evolve and transfer into one another remains poorly understood due to two longstanding challenges. First, the measurements in the two regions are separated by a gap at altitudes ~800–8,000 km. Second, fundamentally different techniques are used to measure plasma densities in the plasmasphere and topside ionosphere. Here, we address both of these issues and show that two of the most prominent N_e measurement approaches in the respective regions—using wave spectra and radio occultations—yield near-identical results. Using observations by the Arase mission at altitudes 440–32,000 km, we demonstrate that it is possible to bridge the gap between the ionosphere and plasmasphere. This result enables studying the dynamics of their transition region and several other fundamental questions about the distribution and life cycle of cold plasma in geospace.

Key Points:

- The first direct comparison of N_e from radio occultations (RO) and upper hybrid resonance (UHR) frequencies shows near-identical agreement (~5% median difference)
- Combining Constellation Observing System for Meteorology, Ionosphere and Climate RO and Arase UHR measurements enables deriving vertical scale height profiles in ionosphere-plasmasphere transition region
- Bridging the gap between ionosphere and plasmasphere enables studying key questions about their interactions, which remain poorly understood

Supporting Information:

Supporting Information may be found in the online version of this article.

Correspondence to:

A. Smirnov,
a.smirnov@lmu.de

Citation:

Smirnov, A., Shprits, Y., Lühr, H., Kronberg, E. A., Goldstein, J., Miyoshi, Y., et al. (2025). Bridging the gap between the Earth's ionosphere and plasmasphere. *Geophysical Research Letters*, *52*, e2025GL119267. https://doi.org/10.1029/2025GL119267

Received 6 SEP 2025
Accepted 17 NOV 2025

Author Contributions:

Conceptualization: Artem Smirnov, Yuri Shprits
Data curation: Artem Smirnov, Yoshizumi Miyoshi, Nicholas Pedatella, Bernhard Haas, Yoshiya Kasahara, Fuminori Tsuchiya, Shoya Matsuda, Atsuki Shinbori, Ayako Matsuoka
Formal analysis: Artem Smirnov, Yuri Shprits, Hermann Lühr, Elena A. Kronberg, Jerry Goldstein, Yoshizumi Miyoshi, Fabricio Prol, Alessio Pignalberi, Natalia Buzulukova,

1. Introduction

The distribution of cold plasma in the ionosphere-plasmasphere system has a controlling effect on a variety of physical phenomena, including wave-particle interactions, coupling processes, and radio wave propagation (Delzanno et al., 2021; Gallagher et al., 2021; Goldstein et al., 2021). The dynamics of the two regions are different but strongly coupled. Ionospheric particles refill the plasmasphere on the dayside, while plasmaspheric particles help sustain the ionosphere at night due to downward ambipolar diffusion (Figure 1a, see also Park (1970)). Despite the importance of the ionosphere-plasmasphere for both scientific and practical

Nicholas Pedatella, Bernhard Haas, Dedong Wang
Funding acquisition: Elena A. Kronberg, Dedong Wang
Investigation: Artem Smirnov, Yuri Shprits, Hermann Lühr, Elena A. Kronberg, Fabricio Prol, Alessio Pignalberi
Methodology: Artem Smirnov, Elena A. Kronberg, Fabricio Prol, Alessio Pignalberi, Natalia Buzulukova, Bernhard Haas
Project administration: Elena A. Kronberg
Resources: Yuri Shprits, Elena A. Kronberg, Yoshizumi Miyoshi, Nicholas Pedatella, Dedong Wang, Yoshiya Kasahara, Fuminori Tsuchiya, Shoya Matsuda, Atsuki Shinbori, Ayako Matsuoka
Software: Artem Smirnov
Supervision: Yuri Shprits, Hermann Lühr, Elena A. Kronberg
Validation: Artem Smirnov, Alessio Pignalberi, Bernhard Haas
Visualization: Artem Smirnov, Elena A. Kronberg, Jerry Goldstein
Writing – original draft: Artem Smirnov
Writing – review & editing: Artem Smirnov, Yuri Shprits, Hermann Lühr, Elena A. Kronberg, Jerry Goldstein, Yoshizumi Miyoshi, Fabricio Prol, Alessio Pignalberi, Natalia Buzulukova, Nicholas Pedatella, Bernhard Haas, Dedong Wang, Yoshiya Kasahara, Fuminori Tsuchiya, Shoya Matsuda, Atsuki Shinbori, Ayako Matsuoka

applications, the data coverage in the two regions remains highly non-uniform (e.g., Smirnov et al., 2021). The available electron density (N_e) measurements are separated by a longstanding observational gap in altitudes from ∼800 to ∼8,000 km (Bilitza et al., 2022; Prol et al., 2022). Due to this gap, it remains uncertain how the ionosphere and plasmasphere populations transfer or evolve into one another, and the N_e distribution in their transition region remains poorly quantified.

An additional complication for combined studies of the ionosphere and plasmasphere arises from the different measurement techniques used in the two regions (Figures 1b and 1c). In the plasmasphere, electron densities are typically calculated from upper hybrid resonance (UHR) frequencies (e.g., Delzanno et al., 2021), while in the topside ionosphere they are primarily obtained from Langmuir Probes and radio occultations (RO) (Pedatella et al., 2015; Smirnov et al., 2021). Currently, RO represents the only active observational technique that allows profiling through the entire F-layer of the ionosphere with global coverage (Cherniak & Zakharenkova, 2014). RO uses Global Navigation Satellite Systems (GNSS) signals to obtain electron density profiles (EDPs), which have shown very good agreement with other data sources and provide three-dimensional views of the ionosphere (Cherniak et al., 2021; Jakowski et al., 2002). Because RO data are confined to altitudes below ∼800 km and UHR N_e observations have been limited to high altitudes above ∼8,000 km, a direct comparison between the two techniques has not been performed, leaving it uncertain whether key data sources in the two regions could be combined or if they have systematic biases or differences.

In this study, we present the first direct comparison between electron densities obtained from UHR frequencies and GNSS RO. We use N_e observations by the Plasma Wave Experiment (PWE) onboard the Arase mission (Kasahara, Kasaba, et al., 2018; Miyoshi et al., 2012). Although Arase is primarily targeted at studying the inner magnetosphere, the frequency limits of its PWE suite are very broad and allow retrieving N_e at altitudes down to ∼440 km, which could not be achieved by previous magnetospheric satellites (Kumamoto et al., 2018). As ionospheric reference measurements, we use RO EDPs from the Constellation Observing System for Meteorology, Ionosphere and Climate (COSMIC) mission (Schreiner et al., 2007). We identify 1,476 conjunctions between Arase and COSMIC during their overlap in 2017–2019 and find excellent agreement between the two data sets, with a near-zero bias of a few percent. Using the combined COSMIC-Arase data set, we show that it is possible to fill in the part of vertical scale height profiles at the ionosphere-plasmasphere transition that remained poorly constrained due to the previous lack of observations. The near-identical correspondence between electron densities obtained from UHR frequencies and GNSS RO opens new opportunities for studying fundamental questions about the coupled ionosphere-plasmasphere dynamics and their transition zone.

2. Data Set

The COSMIC mission, which operated from 2006 to 2019, provided an extensive electron density data set for ionospheric science. The mission consisted of six microsatellites in 72° inclination orbits separated by ∼30° in longitude (Lei et al., 2007). The satellites were equipped with the Global positioning system Occultation eXperiment receivers that allowed retrieving electron densities for both setting and rising occultations for the first time (Schreiner et al., 2007). This helped to provide dense 3D coverage of the ionosphere at heights up to ∼800 km, with over 4.5 million EDPs. The estimated precision of COSMIC electron densities is $\sim 10^3$ cm^{-3} (compared to typical N_e values of $\sim 10^5 - 10^6$ cm^{-3}) and the corresponding spatial (horizontal) resolution is about 300 km (Schreiner et al., 2007). The quality of COSMIC EDPs has been analyzed extensively, showing good agreement with other instruments, including incoherent scatter radars (e.g., Cherniak & Zakharenkova, 2014; Lei et al., 2007), ionosondes (Chuo et al., 2011; Habarulema & Carelse, 2016) and Langmuir probes (Pedatella et al., 2015). Smirnov et al. (2021) demonstrated that COSMIC EDPs provided a robust three-dimensional framework for calibrating other missions in the topside ionosphere, and therefore we use COSMIC RO profiles for validating Arase observations.

Cold-plasma measurements in the inner magnetosphere are notoriously difficult (Delzanno et al., 2021), and using UHR frequencies is widely regarded as the most reliable approach to obtain electron densities (Hartley et al., 2023). JAXA's Arase mission provides electric field wave observations at frequencies from a few Hz up to 10 MHz by means of the Onboard Frequency Analyzer (OFA) and High Frequency Analyzer (HFA), which are part of the PWE suite (Kasahara, Kasaba, et al., 2018; Kumamoto et al., 2018; Matsuda et al., 2018; Miyoshi et al., 2018). Arase has a highly elliptical orbit with a perigee of ∼440 km and apogee of ∼32,000 km (Miyoshi et al., 2018). Electron density along the satellite orbit is derived using the PWE/OFA and HFA instruments and in

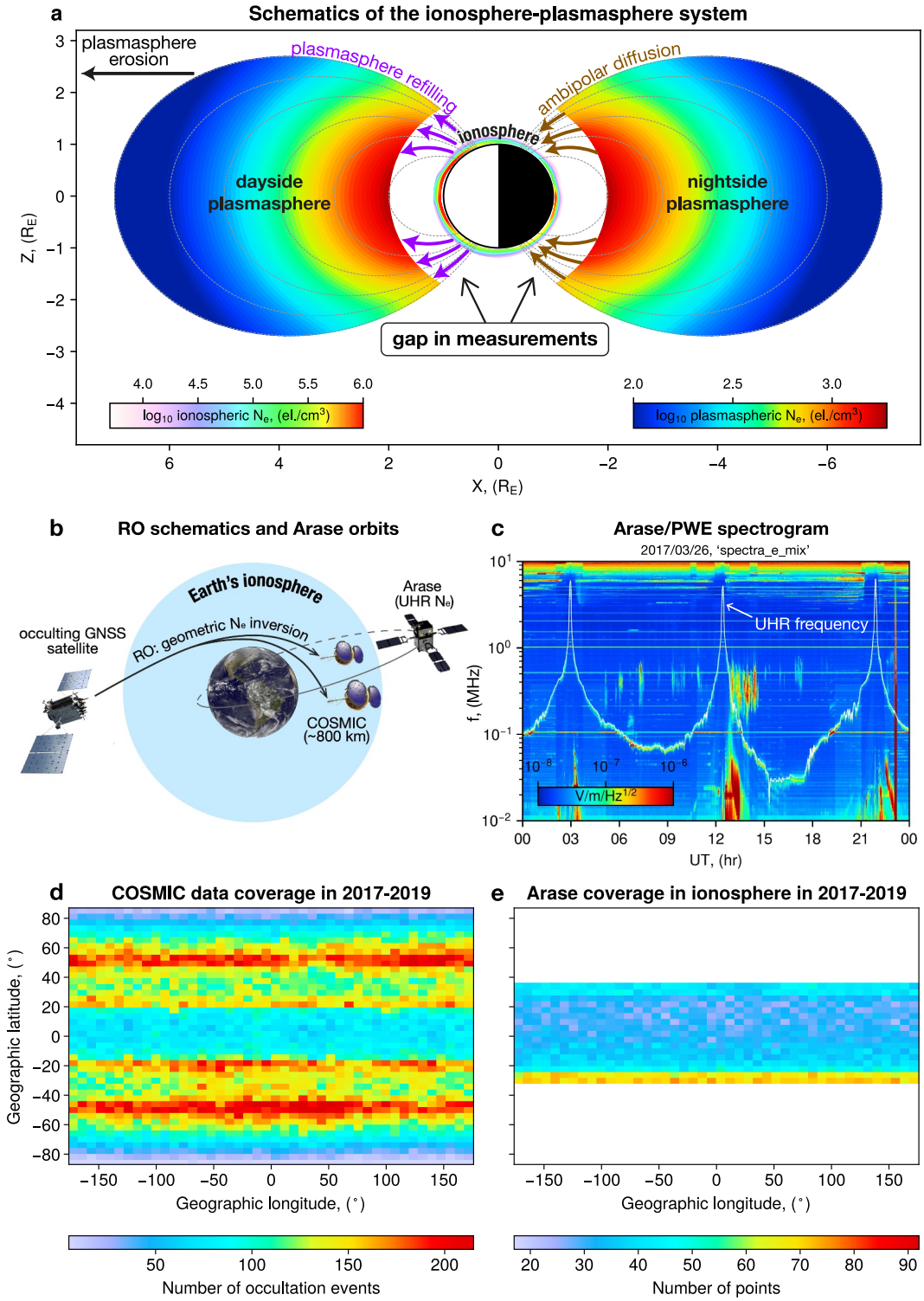

Figure 1. (a) Schematic representation of the ionosphere-plasmasphere system, illustrating the altitude gap in observations between the two regions. The ionospheric distribution is obtained from the Neural network model of Electron density in the Topside ionosphere model (Smirnov et al., 2023), while plasmaspheric N_e are based on the Carpenter and Anderson (1992) model with field-line dependence from Denton et al. (2006). (b) Schematics of the radio occultations technique, inverting N_e from bending angles of Global Navigation Satellite Systems signals. (c) An example of an Arase/Plasma Wave Experiment spectrogram used to infer N_e from upper hybrid resonance frequencies. Panels (d, e) show the geographic coverage of Constellation Observing System for Meteorology, Ionosphere and Climate and Arase observations in the topside ionosphere during their overlap in 2017–2019.

situ magnetic field observations from MGF (Matsuoka et al., 2018). The notable difference between the wave instruments on Arase and those on previous magnetospheric missions is their very high spectral width (Figure 1c), which allows detecting the UHR frequency at very low altitudes, deep within the ionosphere (~440 km). For comparison, the Van Allen Probes mission had instruments that allowed inferring N_e only at altitudes of ~8,000 km and above (Hartley et al., 2023; Kletzing et al., 2013; Zhelavskaya et al., 2017). The Arase measurements are provided with a spatial resolution of about 400 km, roughly similar to that of COSMIC EDPs. Arase N_e measurements were previously compared to the Van Allen Probes observations and used for modeling electron densities around the inner radiation belt (Hartley et al., 2023) and in the broader plasmasphere (Watanabe et al., 2025), but have not yet been utilized for analyzing the topside ionosphere.

In addition to COSMIC observations, we compare Arase measurements with the recently developed Neural network model of Electron density in the Topside ionosphere (NET) (Smirnov et al., 2023). The NET model is driven by a combination of solar flux index P10.7 and geomagnetic indices Kp and SYM-H. It was trained on RO data processed by University Corporation for Atmospheric Research (UCAR) from COSMIC, Gravity Recovery and Climate Experiment (GRACE), CHAllenging Minisatellite Payload (CHAMP) missions, with a recent addition of PlanetIQ observations, and showed very good agreement with several independent observational sources (Schreiter et al., 2024; Smirnov et al., 2023). The model was not trained on Arase measurements and is therefore well suited for an independent evaluation of these data.

3. Comparing Arase Observations to COSMIC Data and NET Model Results

To compare electron density measurements from the COSMIC and Arase missions, we impose spatial and temporal conjunction criteria. We use Arase data at heights below 800 km, in order not to extrapolate COSMIC profiles in altitude. The geographic coverage of the two missions is shown in Figures 1d and 1e. For each COSMIC EDP, we select Arase measurements within ±5° geographic latitude, ±10° longitude, and ±1 hr of universal time. These thresholds are generally within the ionospheric correlation lengths (Forsythe, Azeem, & Crowley, 2020; Forsythe, Azeem, Crowley, Makarevich, & Wang, 2020) and allow us to find a sufficient number of co-locations in 2017–2019. We find 1,476 conjunctions between Arase observations and COSMIC EDPs, and interpolate COSMIC density profiles onto Arase altitudes for comparison. Our results indicate an excellent agreement between the two missions with a very high Spearman rank correlation of 0.93 and low median bias of $-2{,}290$ cm^{-3}, which corresponds to a ~5% difference when normalized to the median COSMIC N_e value (Figures 2a–2c and Table 1). Furthermore, over 93% of electron densities in conjunctions are within a factor of 2 from each other (Figure 2c), which also attests to the very good correspondence between COSMIC and Arase measurements.

Conjunction analyses always rely on limited statistics, and therefore other approaches to data calibration have been proposed. For instance, it is possible to use empirical models for evaluating data sets with unknown baselines (Schreiter et al., 2023; Smirnov et al., 2024). This allows covering a much broader range of conditions without limiting the number of points to physical co-locations. Here, we compare Arase measurements with the NET model (provided in Smirnov (2025)). We use the full Arase data set until December 2023 and run the model along the orbit for time intervals that were not used in model training (Figure 2d). The metrics for Arase-NET comparison are similar to those for the conjunction analysis (Table 1), with a median difference of $-2{,}920$ cm^{-3}. This corresponds to ~−4.7% when normalized to the median electron density value predicted by NET. The corresponding Spearman rank correlation is 0.93, and for 89% of the points Arase measurements and NET predictions fall within a factor of 2 from each other (Figure 2f).

4. Quantifying the Ionosphere-Plasmasphere Transition Region

The ionosphere-plasmasphere transition has remained poorly quantified due to the lack of observations, most of which predate 1983 (see Table 1 in Bilitza et al. (2022)). The combined COSMIC-Arase data set provides an unprecedented opportunity to fill in the missing part of the global electron density distribution. Here, we show that it is possible to seamlessly incorporate these data into joint modeling frameworks by parametrizing radial N_e profiles with an alpha-Chapman function (Chapman, 1931), which is based on first principles and is highly

10.1029/2025GL119267

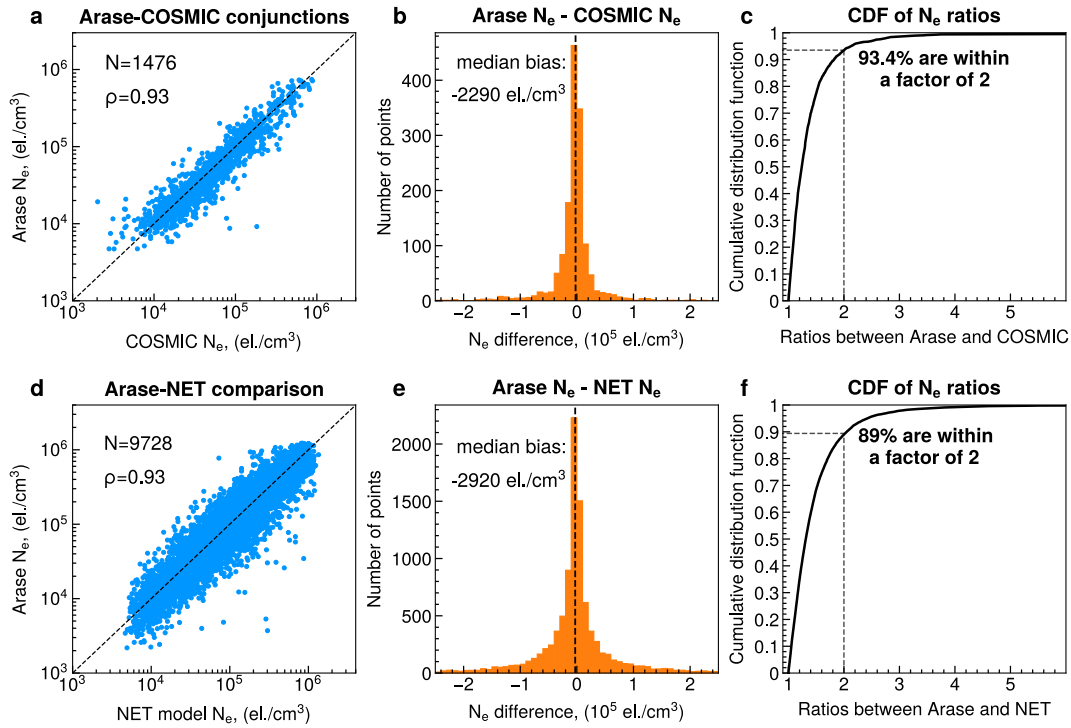

Figure 2. Comparison of Arase measurements to Constellation Observing System for Meteorology, Ionosphere and Climate (COSMIC) observations (top row), and to predictions of the ionospheric Neural network model of Electron density in the Topside ionosphere (NET) model (bottom row). Panel (a) shows a scatter plot of N_e values by COSMIC and Arase missions in conjunctions; subplot (b) shows the histogram of differences between Arase and COSMIC electron densities. Panel (c) shows cumulative distribution function of the ratios between COSMIC and Arase densities (for ratios <1, inverted values are taken). The bottom row is in the same format, except for the COSMIC-NET comparison. Arase data agree well both with COSMIC measurements, with 93.4% of N_e values in conjunctions being within a factor of 2 from each other, and with NET predictions (89% of points within a factor of 2).

effective for describing vertical changes of electron density (Fonda et al., 2005; Hernández-Pajares et al., 2017; Prol et al., 2018, 2019; Smirnov et al., 2023).

The alpha-Chapman function is a mathematical expression that describes electron density (N_e) variations with altitude (h) as follows:

Table 1
Metrics for Comparisons Between Arase Observations to Constellation Observing System for Meteorology, Ionosphere and Climate Data and Neural Network Model of Electron Density in the Topside Ionosphere Model Results

Metric	Arase-COSMIC comparison	Arase-NET comparison
Median difference, (cm^{-3})	−2,290	−2,920
Normalized median difference, (%)	−5.1	−4.1
Median logarithmic difference	−0.07	−0.08
Mean difference, (cm^{-3})	−5,569	−6,958
Normalized mean difference, (%)	−6.8	−4.7
Mean logarithmic difference	−0.07	−0.08
Standard deviation of the differences, (cm^{-3})	41,742	93,784
Normalized standard deviation of the differences, (%)	51	64
Percent of values within a factor of 2	93.4	89
Percent of values within a factor of 5	99.5	99.7
Spearman correlation (ρ)	0.93	0.93

$$\begin{cases} N_e(h) = \mathrm{NmF2} \cdot \exp(0.5(1 - z - \exp(-z))), \\ z = \dfrac{h - \mathrm{hmF2}}{H_s(h)}, \end{cases} \quad (1)$$

where NmF2 and hmF2 denote the peak electron density and height of the F2-layer. H_s represents an effective scale height, which is defined as a vertical distance over which electron density decreases e times and acts as a shape factor for the density profiles (Rishbeth & Garriott, 1969). It has been shown that an accurate H_s representation is key for reproducing electron density values above the F2-layer peak (Pignalberi et al., 2025; Smirnov et al., 2023; Themens et al., 2018).

There are several ways to estimate alpha-Chapman scale heights. For instance, it is possible to retrieve approximated H_s values from RO or topside sounder EDPs using the Taylor expansion of Equation 1 (Limberger et al., 2013), iterative fitting algorithms (Hernández-Pajares et al., 2017; Prol et al., 2018, 2019) or non-linear least squares (Smirnov et al., 2023). However, the provided solutions are non-unique and sometimes lead to negative scale heights in the topside. Furthermore, they generally require full profiles of N_e and cannot be used to extract H_s from individual measurements. To invert Equation 1, we transform it to the form $W \cdot e^W = \text{const}$ (full derivation is presented in Supporting Information S1). This canonical form allows applying the Lambert-W function (Corless et al., 1996). It is a root-finding technique that yields a solution for H_s given that NmF2 and hmF2 are known. The Lambert-W function has 2 branches (see Figure S1a in Supporting Information S1), and due to the positivity of scale heights above the F2-peak, we use the so-called "main" branch (denoted as W_0) and express the scale height as follows:

$$H_s(h) = \frac{h - \mathrm{hmF2}}{C + W_0(-e^{-C})}, \quad (2)$$

with $C = 1 - 2\ln[N_e(h)/\mathrm{NmF2}]$.

We calculate effective scale heights for the full COSMIC and Arase data sets using Equation 2. This calculation requires knowledge of the F2-peak parameters. For COSMIC, we obtain them directly from the EDPs, while for Arase they are calculated from the NET model. It should be noted that vertical scale heights derived from COSMIC and Arase observations have different meanings. In the topside ionosphere, electrons are mainly supplied from lower altitudes, and H_s reflects the vertical N_e changes due to transport processes such as electromagnetic drifts and ambipolar diffusion (Duncan, 1956; Martyn, 1956; Pignalberi, Pezzopane, Nava, & Coïsson, 2020). In the plasmasphere, particles are generally supplied along the magnetic field lines, and in this case, H_s is not related to the ambipolar diffusion theory and represents an empirical parameter describing electron density decay with radial distance, similar to other exponential N_e parametrizations (e.g., Carpenter & Anderson, 1992). In this study, we quantify H_s in the magnetic equatorial plane and restrict the selected data to quasi-dipole latitudes of ±7.5°, while electron density distributions at higher latitudes can be a topic of future studies.

To investigate how scale heights vary with altitude, we plot H_s occurrences as functions of height (Figure 3). We normalize H_s occurrences to the maximum counts in the respective altitude bins, shown as gray dots. Vertical scale heights calculated from COSMIC generally show a linear dependence on altitude, both on the day- and night-side (Figures 3a and 3c). The spread of values on the dayside is higher at lower altitudes, while on the night-side it increases with height.

In the plasmasphere, scale heights show a quadratic dependence on altitude (Figures 3b and 3d). For comparison, we plot extrapolated linear trends based on COSMIC data in magenta lines. With increasing altitude, the linear trends start to diverge from the data, particularly on the dayside (Figure 3b). This discrepancy can be seen already at ∼2,500 km above hmF2, and at higher altitudes starting from ∼5,000 km the COSMIC trend completely misses the H_s occurrences seen by Arase. For instance, at an altitude of 15,000 km the extrapolated COSMIC trend overestimates the data by ∼40%. Adding Arase data helps to constrain the combined scale height trends (shown in bold gray lines in Figures 3b and 3d) both in the ionosphere-plasmasphere transition and at higher altitudes.

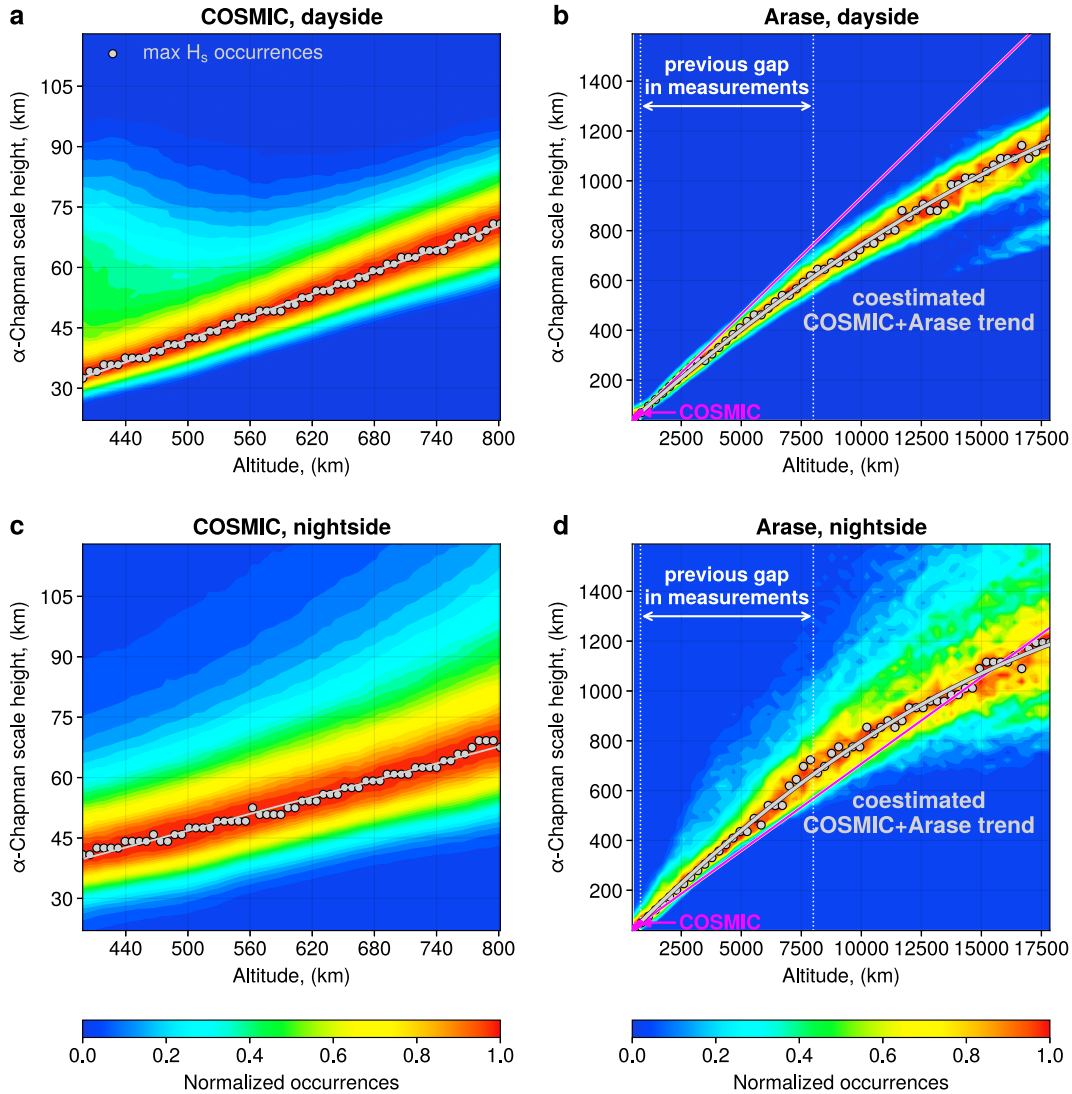

Figure 3. Distribution of scale height values with respect to altitude, derived from Constellation Observing System for Meteorology, Ionosphere and Climate (COSMIC) radio occultation measurements (left column) and Arase (right column). The color-coded values are normalized to the maxima in each altitude bin, shown in gray dots. For COSMIC data, we fit linear trends to scale heights, while at Arase the H_s dependence on altitude becomes quadratic (thick gray line in panels (b, d)). Extrapolation of ionospheric profiles to high altitudes (magenta lines) leads to large discrepancies on the dayside, overestimating plasmaspheric scale heights by roughly 40% (panel (b)). Including Arase data helps to constrain the trend estimation and prevent artifacts.

5. Discussion and Conclusions

Two longstanding challenges have greatly restricted our ability to study the ionosphere and plasmasphere as a coupled system. First, a large observational gap separated the available measurements in the two regions. Second, the available observations were conducted using vastly different techniques that had not been compared. Here, we address both issues and show that two of the most widely used approaches for measuring N_e, namely, using GNSS RO in the ionosphere and UHR frequencies in the plasmasphere, yield near-identical results. This bridges the gap between the two regions and enables studying the dynamics of their transition region, which remained poorly understood due to the prior lack of observations.

By comparing Arase and COSMIC observations, we find that electron densities calculated from UHR frequencies and GNSS RO are in excellent agreement with a median difference of ∼5% and correlation of 0.93. This is particularly striking given the fundamentally different nature of the two techniques (Figures 1b and 1c). While RO

obtains electron densities from the geometric inversion of GNSS signals (Schreiner et al., 2007), UHR N_e are calculated from plasma wave spectra (Kumamoto et al., 2018). The fact that the two methods show such high consistency indicates the robustness of both techniques for measuring plasma densities. Previous studies devoted to cross-calibration of N_e measurements have focused on comparing missions that operated within a single region of geospace (Cherniak & Zakharenkova, 2014; Hartley et al., 2023; Lei et al., 2007; Pedatella et al., 2015; Smirnov et al., 2021, 2024). Unlike the previous magnetospheric missions, Arase samples electron densities at altitudes of $\sim 440 - 32000$ km, which allows comparing the data across the ionosphere-plasmasphere system. Our results extend to other missions that have already been shown to agree with COSMIC and Arase, such as the GRACE, CHAMP, Communication/Navigation Outage Forecasting System (C/NOFS), Swarm, and Van Allen Probes, and allow establishing a new framework of well-calibrated observations for studying the cold plasma distribution in near-Earth space (Hartley et al., 2023; Pedatella et al., 2015; Smirnov et al., 2021, 2024).

Arase data can help to significantly advance empirical modeling of the ionosphere-plasmasphere system. The existing models have either used separate parametrizations of the two regions, interpolated N_e across the data gap, or extrapolated ionospheric profiles into the plasmasphere (for details, see Gallagher et al. (2000), Stankov and Jakowski (2006), Nava et al. (2008), Prol et al. (2022), Pezzopane et al. (2024), and references therein). Each of these approaches carries substantial uncertainty (Prol et al., 2022). Consequently, a lot of recent emphasis has been made on improving the integration of prominent ionospheric models, such as the International Reference Ionosphere (Bilitza et al., 2022) and NeQuick (Nava et al., 2008; Pezzopane et al., 2024), with plasmaspheric models (Bilitza et al., 2024; Watanabe et al., 2025). We demonstrate that key data sets in the two regions can be combined directly, without the need for further calibration. Using the alpha-Chapman function, we provide a simple way to incorporate these data into joint modeling frameworks. Our results indicate that, particularly on the dayside, ionospheric observations provide too little altitude coverage to infer the full N_e profiles (Figure 3b), and additional data at high altitudes are necessary to prevent extrapolation artifacts in empirical models (see also Pignalberi et al. (2021) and Prol et al. (2022)). The Arase data set is well suited for this task, and can additionally be used for analyzing the asymptotic parameters of models based on the NeQuick formulation (Pignalberi, Pezzopane, Themens, et al., 2020).

Physics-based models of the plasmasphere typically set inner-boundary conditions at altitudes of 800–3,000 km (Pierrard & Voiculescu, 2011; Pierrard et al., 2021; Zhelavskaya et al., 2021). Other modeling approaches, such as the 3D magnetohydrodynamic (MHD) model of the ionosphere-plasmasphere system SAMI3 (Huba & Krall, 2013; Huba & Liu, 2023) require data sets in the "gap" region to validate model performance. Improving electron density coverage at the respective altitudes can significantly enhance the results of these physics-based codes. Furthermore, global MHD frameworks for simulations of the magnetosphere are coupled with electrodynamic ionospheric solvers, and need to specify background plasma parameters at the inner boundary of the simulations, typically around 2–3 R_E. The inner MHD boundary serves as an interface between magnetospheric and ionospheric solutions. According to the summary of boundary conditions provided by Xi et al. (2015), a number of MHD models assume fixed and activity independent N_e values at the boundary, ranging from 2 cm^{-3} (OpenGGCM code, Raeder, 2003) to 28 cm^{-3} (SWMF code, Welling & Liemohn, 2014), and 370 cm^{-3} (PPMLR code, Hu et al., 2007). Incorporating realistic electron density estimates would allow MHD models to move beyond static boundary assumptions and better reproduce global magnetospheric dynamics. Cold plasma density also enters the equation for Alfvenic speed. Therefore, N_e distribution influences propagation of MHD waves, both in Alfvenic and magnetosonic modes, and is essential to understand global dynamics of ULF waves (Hartinger et al., 2014, 2015) and for studies of compressional disturbances (Fujita et al., 2003).

Cold plasma of ionospheric origin plays a critical role in global magnetospheric dynamics. For instance, electron density in the plasmasphere controls generation of waves and wave-particle interactions, affecting energization and loss of plasma in the radiation belts and ring current (e.g., Li & Hudson, 2019). Additionally, plasmaspheric plumes influence the electrodynamics and rates of reconnection at the dayside magnetopause (Delzanno et al., 2021; Kronberg et al., 2021; Toledo-Redondo et al., 2021). Despite the importance of cold plasma, several fundamental questions regarding its life cycle remain unanswered. Although it is well established that ionospheric plasma refills the plasmasphere, our understanding of this process is far from complete (Gallagher & Comfort, 2016; Goldstein et al., 2019, 2021). Additionally, with increasing altitude the governing physical processes change. The ionosphere is strongly influenced by interactions with the neutral atmosphere, while the plasmaspheric morphology is mainly determined by electric and magnetic field configurations. The processes at the

transition between these two regimes, however, remain uncertain. It is, for example, not well understood at which altitude the influence of geographic longitude on the plasma distribution ceases. Our results provide a crucial step toward studying these fundamental questions and open many opportunities for further investigations. They also indicate that additional dedicated missions are needed to fully characterize the dynamics and evolution of cold plasma in the near-Earth space environment.

Conflict of Interest

The authors declare no conflicts of interest relevant to this study.

Data Availability Statement

All data used in this study are publicly available. COSMIC data are available at UCAR COSMIC Program (2022). Arase PWE/HFA data, produced by the ERG Science Center (https://ergsc.isee.nagoya-u.ac.jp/data_info/erg.shtml.en), are provided at Kasahara, Kumamoto, et al. (2018), and Kasahara et al. (2021).

Acknowledgments

A. S. is supported by Deutsche Forschungsgemeinschaft (DFG), Project 520916080. E. A. K. is supported by the DFG Heisenberg Grant 516641019. F. P. is supported by the Research Council of Finland under the project "Exploring the Upper Limits of the Ionosphere (EULI)," under Decision 362096. This material is based upon work supported by the NSF National Center for Atmospheric Research, which is a major facility sponsored by the U.S. National Science Foundation under Cooperative Agreement 1852977. N. P. acknowledges support from U.S. National Science Foundation Grant AGS-2054356. N. B. was supported by NASA Living with a Star Targeted Research and Technology Program under Work Breakdown Structure (WBS) 936723.02.01.12.75, and by Partnership for Heliophysics and Space Environment Research (PHaSER), NASA Cooperative Agreement 80NSSC21M0180. A. S. is grateful to Alwin Roy (GFZ) for the help with preparing Figure 1c. The authors acknowledge support from the International Space Science Institute (ISSI-Bern, Switzerland) through the ISSI Working Group on "Advancing the topside ionosphere and lower plasmasphere modeling". Open Access funding enabled and organized by Projekt DEAL.

References

Bilitza, D., Pezzopane, M., Truhlik, V., Altadill, D., Reinisch, B. W., & Pignalberi, A. (2022). The International Reference Ionosphere model: A review and description of an ionospheric benchmark. *Reviews of Geophysics*, *60*(4), e2022RG000792. https://doi.org/10.1029/2022rg000792

Bilitza, D., Truhlik, V., Yoshihara, O., & Moldwin, M. B. (2024). Development and improvement of the International Reference Ionosphere with special emphasis on the topside and extension to the plasmasphere. *Annals of Geophysics*, *67*(4), SA443. https://doi.org/10.4401/ag-9145

Carpenter, D., & Anderson, R. (1992). An ISEE/whistler model of equatorial electron density in the magnetosphere. *Journal of Geophysical Research*, *97*(A2), 1097–1108. https://doi.org/10.1029/91JA01548

Chapman, S. (1931). The absorption and dissociative or ionizing effect of monochromatic radiation in an atmosphere on a rotating Earth. *Proceedings of the Physical Society*, *43*(1), 26–45. https://doi.org/10.1088/0959-5309/43/1/305

Cherniak, I. V., & Zakharenkova, I. (2014). Validation of FORMOSAT-3/COSMIC radio occultation electron density profiles by incoherent scatter radar data. *Advances in Space Research*, *53*(9), 1304–1312. https://doi.org/10.1016/j.asr.2014.02.010

Cherniak, I. V., Zakharenkova, I., Braun, J., Wu, Q., Pedatella, N., Schreiner, W., et al. (2021). Accuracy assessment of the quiet-time ionospheric F2 peak parameters as derived from COSMIC-2 multi-GNSS radio occultation measurements. *Journal of Space Weather and Space Climate*, *11*, 18. https://doi.org/10.1051/swsc/2020080

Chuo, Y.-J., Lee, C.-C., Chen, W.-S., & Reinisch, B. W. (2011). Comparison between bottomside ionospheric profile parameters retrieved from FORMOSAT3 measurements and ground-based observations collected at Jicamarca. *Journal of Atmospheric and Solar-Terrestrial Physics*, *73*(13), 1665–1673. https://doi.org/10.1016/j.jastp.2011.02.021

Corless, R. M., Gonnet, G. H., Hare, D. E., Jerey, D. J., & Knuth, D. E. (1996). On the Lambert W function. *Advances in Computational Mathematics*, *5*(1), 329–359. https://doi.org/10.1007/bf02124750

Delzanno, G. L., Borovsky, J. E., Henderson, M. G., Lira, P. A. R., Roytershteyn, V., & Welling, D. T. (2021). The impact of cold electrons and cold ions in magnetospheric physics. *Journal of Atmospheric and Solar-Terrestrial Physics*, *220*, 105599. https://doi.org/10.1016/j.jastp.2021.105599

Denton, R., Takahashi, K., Galkin, I., Nsumei, P., Huang, X., Reinisch, B., et al. (2006). Distribution of density along magnetospheric field lines. *Journal of Geophysical Research*, *111*(A4), A04213. https://doi.org/10.1029/2005JA011414

Duncan, R. (1956). The behaviour of a Chapman layer in the night F2 region of the ionosphere, under the influence of gravity, diffusion, and attachment. *Australian Journal of Physics*, *9*(4), 436–439.

Fonda, C., Coïsson, P., Nava, B., & Radicella, S. M. (2005). Comparison of analytical functions used to describe topside electron density profiles with satellite data. *Annals of Geophysics*, *48*(3).

Forsythe, V. V., Azeem, I., & Crowley, G. (2020). Ionospheric horizontal correlation distances: Estimation, analysis, and implications for ionospheric data assimilation. *Radio Science*, *55*(12), 114. https://doi.org/10.1029/2020rs007159

Forsythe, V. V., Azeem, I., Crowley, G., Makarevich, R. A., & Wang, C. (2020). The global analysis of the ionospheric correlation time and its implications for ionospheric data assimilation. *Radio Science*, *55*(12), 110. https://doi.org/10.1029/2020rs007181

Fujita, S., Tanaka, T., Kikuchi, T., Fujimoto, K., Hosokawa, K., & Itonaga, M. (2003). A numerical simulation of the geomagnetic sudden commencement: 1. Generation of the field-aligned current associated with the preliminary impulse. *Journal of Geophysical Research*, *108*(A12), 1416. https://doi.org/10.1029/2002JA009407

Gallagher, D. L., & Comfort, R. (2016). Unsolved problems in plasmasphere refilling. *Journal of Geophysical Research: Space Physics*, *121*(2), 1447–1451. https://doi.org/10.1002/2015JA022279

Gallagher, D. L., Comfort, R., Katus, R., Sandel, B. R., Fung, S. F., & Adrian, M. L. (2021). The breathing plasmasphere: Erosion and refilling. *Journal of Geophysical Research: Space Physics*, *126*(4), e2020JA028727. https://doi.org/10.1029/2020ja028727

Gallagher, D. L., Craven, P. D., & Comfort, R. H. (2000). Global core plasma model. *Journal of Geophysical Research*, *105*(A8), 18819–18833. https://doi.org/10.1029/1999ja000241

Goldstein, J., Gallagher, D. L., Molyneux, P., & Reeves, G. D. (2021). Core-plasma refilling and erosion: Science justification. In *Heliophysics 2050*.

Goldstein, J., Pascuale, S., & Kurth, W. (2019). Epoch-based model for stormtime plasmapause location. *Journal of Geophysical Research: Space Physics*, *124*(6), 4462–4491. https://doi.org/10.1029/2018ja025996

Habarulema, J. B., & Carelse, S. A. (2016). Long-term analysis between radio occultation and ionosonde peak electron density and height during geomagnetic storms. *Geophysical Research Letters*, *43*(9), 4106–4111. https://doi.org/10.1002/2016gl068944

Hartinger, M., Plaschke, F., Archer, M., Welling, D., Moldwin, M., & Ridley, A. (2015). The global structure and time evolution of dayside magnetopause surface eigenmodes. *Geophysical Research Letters*, *42*(8), 2594–2602. https://doi.org/10.1002/2015gl063623

Hartinger, M., Welling, D., Viall, N. M., Moldwin, M. B., & Ridley, A. (2014). The effect of magnetopause motion on fast mode resonance. *Journal of Geophysical Research: Space Physics*, *119*(10), 8212–8227. https://doi.org/10.1002/2014JA020401

Hartley, D., Cunningham, G., Ripoll, J.-F., Malaspina, D., Kasahara, Y., Miyoshi, Y., et al. (2023). Using Van Allen Probes and Arase observations to develop an empirical plasma density model in the inner zone. *Journal of Geophysical Research: Space Physics*, *128*(3), e2022JA031012. https://doi.org/10.1029/2022ja031012

Hernández-Pajares, M., Garcia-Fernàndez, M., Rius, A., Notarpietro, R., von Engeln, A., Olivares-Pulido, G., et al. (2017). Electron density extrapolation above F2 peak by the linear Vary-Chap model supporting new global navigation satellite Systems-LEO occultation missions. *Journal of Geophysical Research: Space Physics*, *122*(8), 9003–9014. https://doi.org/10.1002/2017JA023876

Hu, Y., Guo, X., & Wang, C. (2007). On the ionospheric and reconnection potentials of the Earth: Results from global MHD simulations. *Journal of Geophysical Research*, *112*(A7), A07215. https://doi.org/10.1029/2006ja012145

Huba, J., & Krall, J. (2013). Modeling the plasmasphere with SAMI3. *Geophysical Research Letters*, *40*(1), 6–10. https://doi.org/10.1029/2012gl054300

Huba, J., & Liu, H.-L. (2023). Modeling the development of plasmasphere ducts and irregularities with SAMI3/WACCM-X. *Geophysical Research Letters*, *50*(20), e2023GL105470. https://doi.org/10.1029/2023gl105470

Jakowski, N., Wehrenpfennig, A., Heise, S., Reigber, C., Lühr, H., Grunwaldt, L., & Meehan, T. (2002). GPS radio occultation measurements of the ionosphere from CHAMP: Early results. *Geophysical Research Letters*, *29*(10), 951. https://doi.org/10.1029/2001gl014364

Kasahara, Y., Kasaba, Y., Kojima, H., Yagitani, S., Ishisaka, K., Kumamoto, A., et al. (2018). The plasma wave experiment (PWE) on board the Arase (ERG) satellite. *Earth Planets and Space*, *70*(1), 86. https://doi.org/10.1186/s40623-018-0842-4

Kasahara, Y., Kumamoto, A., Tsuchiya, F., Kojima, H., Matsuda, S., Matsuoka, A., et al. (2021). The PWE/HFA instrument Level-3 electron density data of exploration of energization and radiation in geospace (ERG) Arase satellite [Dataset]. https://doi.org/10.34515/DATA.ERG-10001

Kasahara, Y., Kumamoto, A., Tsuchiya, F., Matsuda, S., Shoji, M., Nakamura, S., et al. (2018). The PWE/HFA instrument level-2 spectrum data of exploration of energization and radiation in geospace (ERG) Arase satellite [Dataset]. https://doi.org/10.34515/DATA.ERG-10000

Kletzing, C., Kurth, W., Acuna, M., MacDowall, R., Torbert, R., Averkamp, T., et al. (2013). The electric and magnetic field instrument suite and integrated science (EMFISIS) on RBSP. *Space Science Reviews*, *179*(1), 127–181. https://doi.org/10.1007/s11214-013-9993-6

Kronberg, E. A., Grigorenko, E. E., Ilie, R., Kistler, L., & Welling, D. (2021). Impact of ionospheric ions on magnetospheric dynamics. *Magnetospheres in the Solar System*, 353–364. https://doi.org/10.1002/9781119815624.ch23

Kumamoto, A., Tsuchiya, F., Kasahara, Y., Kasaba, Y., Kojima, H., Yagitani, S., et al. (2018). High frequency analyzer (HFA) of plasma wave experiment (PWE) onboard the Arase spacecraft. *Earth Planets and Space*, *70*(1), 114. https://doi.org/10.1186/s40623-018-0854-0

Lei, J., Syndergaard, S., Burns, A. G., Solomon, S. C., Wang, W., Zeng, Z., et al. (2007). Comparison of COSMIC ionospheric measurements with ground-based observations and model predictions: Preliminary results. *Journal of Geophysical Research*, *112*(A7), A07308. https://doi.org/10.1029/2006ja012240

Li, W., & Hudson, M. (2019). Earth's Van Allen radiation belts: From discovery to the Van Allen Probes era. *Journal of Geophysical Research: Space Physics*, *124*(11), 8319–8351. https://doi.org/10.1029/2018ja025940

Limberger, M., Liang, W., Schmidt, M., Dettmering, D., & Hugentobler, U. (2013). Regional representation of F2 Chapman parameters based on electron density profiles. *Annales Geophysicae*, *31*, 2215–2227. https://doi.org/10.5194/angeo-31-2215-2013

Martyn, D. (1956). Processes controlling ionization distribution in the F2 region of the ionosphere. *Australian Journal of Physics*, *9*(1), 161–166. https://doi.org/10.1071/ph560161

Matsuda, S., Kasahara, Y., Kojima, H., Kasaba, Y., Yagitani, S., Ozaki, M., et al. (2018). Onboard software of plasma wave experiment aboard Arase: Instrument management and signal processing of waveform capture/onboard frequency analyzer. *Earth Planets and Space*, *70*(1), 122. https://doi.org/10.1186/s40623-018-0838-0

Matsuoka, A., Teramoto, M., Nomura, R., Nosé, M., Fujimoto, A., Tanaka, Y., et al. (2018). The ARASE (ERG) magnetic field investigation. *Earth Planets and Space*, *70*(1), 116. https://doi.org/10.1186/s40623-018-0800-1

Miyoshi, Y., Ono, T., Takashima, T., Asamura, K., Hirahara, M., Kasaba, Y., et al. (2012). The energization and radiation in geospace (ERG) project. *Geophysical Monograph Series*, *199*, 103116. https://doi.org/10.1029/2012GM001304

Miyoshi, Y., Shinohara, I., Takashima, T., Asamura, K., Higashio, N., Mitani, T., et al. (2018). Geospace exploration project ERG. *Earth Planets and Space*, *70*(1), 101. https://doi.org/10.1186/s40623-018-0862-0

Nava, B., Coisson, P., & Radicella, S. (2008). A new version of the NeQuick ionosphere electron density model. *Journal of Atmospheric and Solar-Terrestrial Physics*, *70*(15), 1856–1862. https://doi.org/10.1016/j.jastp.2008.01.015

Park, C. (1970). Whistler observations of the interchange of ionization between the ionosphere and the protonosphere. *Journal of Geophysical Research*, *75*(22), 4249–4260. https://doi.org/10.1029/ja075i022p04249

Pedatella, N., Yue, X., & Schreiner, W. (2015). Comparison between GPS radio occultation electron densities and in situ satellite observations. *Radio Science*, *50*(6), 518–525. https://doi.org/10.1002/2015rs005677

Pezzopane, M., Pignalberi, A., Pietrella, M., Haralambous, H., Prol, F., Nava, B., et al. (2024). An update of the NeQuick-Corr topside ionosphere modeling based on new datasets. *Atmosphere*, *15*(4), 498. https://doi.org/10.3390/atmos15040498

Pierrard, V., Botek, E., & Darrouzet, F. (2021). Improving predictions of the 3D dynamic model of the plasmasphere. *Frontiers in Astronomy and Space Sciences*, *8*, 681401. https://doi.org/10.3389/fspas.2021.681401

Pierrard, V., & Voiculescu, M. (2011). The 3D model of the plasmasphere coupled to the ionosphere. *Geophysical Research Letters*, *38*(12), L12104. https://doi.org/10.1029/2011gl047767

Pignalberi, A., Bilitza, D., Coïsson, P., Haralambous, H., Nava, B., Pezzopane, M., et al. (2025). Validation of the IRI-2020 topside ionosphere options through in-situ electron density observations by low-earth-orbit satellites. *Advances in Space Research*, *75*(5), 4192–4216. https://doi.org/10.1016/j.asr.2024.05.056

Pignalberi, A., Pezzopane, M., & Nava, B. (2021). Optimizing the NeQuick topside scale height parameters through COSMIC/FORMOSAT-3 radio occultation data. *IEEE Geoscience and Remote Sensing Letters*, *19*, 1–5. https://doi.org/10.1109/lgrs.2021.3096657

Pignalberi, A., Pezzopane, M., Nava, B., & Coïsson, P. (2020). On the link between the topside ionospheric effective scale height and the plasma ambipolar diffusion, theory and preliminary results. *Scientific Reports*, *10*(1), 17541. https://doi.org/10.1038/s41598-020-73886-4

Pignalberi, A., Pezzopane, M., Themens, D. R., Haralambous, H., Nava, B., & Coïsson, P. (2020). On the analytical description of the topside ionosphere by NeQuick: Modeling the scale height through COSMIC/FORMOSAT-3 selected data. *IEEE Journal of Selected Topics in Applied Earth Observations and Remote Sensing*, *13*, 1867–1878. https://doi.org/10.1109/jstars.2020.2986683

Prol, F. S., Hernández-Pajares, M., Camargo, P. D. O., & Muella, M. T. D. A. H. (2018). Spatial and temporal features of the topside ionospheric electron density by a new model based on GPS radio occultation data. *Journal of Geophysical Research: Space Physics*, *123*(3), 2104–2115. https://doi.org/10.1002/2017JA024936

Prol, F. S., Smirnov, A. G., Hoque, M. M., & Shprits, Y. Y. (2022). Combined model of topside ionosphere and plasmasphere derived from radio-occultation and Van Allen Probes data. *Scientific Reports*, *12*(1), 111. https://doi.org/10.1038/s41598-022-13302-1

Prol, F. S., Themens, D. R., Hernández-Pajares, M., de Oliveira Camargo, P., & Muella, M. T. D. A. H. (2019). Linear Vary-Chap topside electron density model with topside sounder and radio-occultation data. *Surveys in Geophysics*, *40*(2), 277–293. https://doi.org/10.1007/s10712-019-09521-3

Raeder, J. (2003). Global magnetohydrodynamics-a tutorial. *Space Plasma Simulation*, 212–246. https://doi.org/10.1007/3-540-36530-3_11

Rishbeth, H., & Garriott, O. K. (1969). Introduction to ionospheric physics. *Introduction to ionospheric physics*.

Schreiner, W., Rocken, C., Sokolovskiy, S., Syndergaard, S., & Hunt, D. (2007). Estimates of the precision of GPS radio occultations from the COSMIC/FORMOSAT-3 mission. *Geophysical Research Letters*, *34*(4), L04808. https://doi.org/10.1029/2006gl027557

Schreiter, L., Brack, A., Männel, B., Schuh, H., Arnold, D., & Jäggi, A. (2024). Imaging of the ionosphere and plasmasphere using GNSS slant TEC obtained from LEO satellites. *Radio Science*, *59*(12), 119. https://doi.org/10.1029/2024RS008058

Schreiter, L., Stolle, C., Rauberg, J., Kervalishvili, G., van den Ijssel, J., Arnold, D., et al. (2023). Topside ionosphere sounding from the CHAMP, GRACE, and GRACE-FO missions. *Radio Science*, *58*(3), 115. https://doi.org/10.1029/2022rs007552

Smirnov, A. (2025). Model files and example script for the Neural network model of Electron density in the Topside ionosphere (NET), v1.2. *Zenodo*. https://doi.org/10.5281/zenodo.17460567

Smirnov, A., Shprits, Y., Lühr, H., Pignalberi, A., & Xiong, C. (2024). Calibration of Swarm plasma densities overestimation using neural networks. *Space Weather*, *22*(8), e2024SW003925. https://doi.org/10.1029/2024sw003925

Smirnov, A., Shprits, Y., Prol, F., Lühr, H., Berrendorf, M., Zhelavskaya, I., & Xiong, C. (2023). A novel neural network model of Earth's topside ionosphere. *Scientific Reports*, *13*(1), 1303. https://doi.org/10.1038/s41598-023-28034-z

Smirnov, A., Shprits, Y., Zhelavskaya, I., Lühr, H., Xiong, C., Goss, A., et al. (2021). Intercalibration of the plasma density measurements in Earth's topside ionosphere. *Journal of Geophysical Research: Space Physics*, *126*(10), e2021JA029334. https://doi.org/10.1029/2021ja029334

Stankov, S., & Jakowski, N. (2006). Topside ionospheric scale height analysis and modelling based on radio occultation measurements. *Journal of Atmospheric and Solar-Terrestrial Physics*, *68*(2), 134–162. https://doi.org/10.1016/j.jastp.2005.10.003

Themens, D. R., Jayachandran, P., Bilitza, D., Erickson, P. J., Häggström, I., Lyashenko, M. V., et al. (2018). Topside electron density representations for middle and high latitudes: A topside parameterization for E-CHAIM based on the NeQuick. *Journal of Geophysical Research: Space Physics*, *123*(2), 1603–1617. https://doi.org/10.1002/2017ja024817

Toledo-Redondo, S., André, M., Aunai, N., Chappell, C. R., Dargent, J., Fuselier, S., et al. (2021). Impacts of ionospheric ions on magnetic reconnection and Earth's magnetosphere dynamics.

UCAR COSMIC Program. (2022). COSMIC-1 data products [Dataset]. https://doi.org/10.5065/ZD80-KD74

Watanabe, S., Bilitza, D., Tsuchiya, F., Kumamoto, A., Miyoshi, Y., Kasahara, Y., et al. (2025). Satellite observations and modeling of the plasmapause structure and dynamics. *Advances in Space Research*, *75*(5), 4230–4244. https://doi.org/10.1016/j.asr.2024.10.015

Welling, D., & Liemohn, M. (2014). Outflow in global magnetohydrodynamics as a function of a passive inner boundary source. *Journal of Geophysical Research: Space Physics*, *119*(4), 2691–2705. https://doi.org/10.1002/2013JA019374

Xi, S., Lotko, W., Zhang, B., Brambles, O., Lyon, J., Merkin, V., & Wiltberger, M. (2015). Poynting flux-conserving low-altitude boundary conditions for global magnetospheric models. *Journal of Geophysical Research: Space Physics*, *120*(1), 384–400. https://doi.org/10.1002/2014JA020470

Zhelavskaya, I. S., Aseev, N., & Shprits, Y. (2021). A combined neural network- and physics-based approach for modeling plasmasphere dynamics. *Journal of Geophysical Research: Space Physics*, *126*(3), e2020JA028077. https://doi.org/10.1029/2020ja028077

Zhelavskaya, I. S., Shprits, Y. Y., & Spasojević, M. (2017). Empirical modeling of the plasmasphere dynamics using neural networks. *Journal of Geophysical Research: Space Physics*, *122*(11), 11227. https://doi.org/10.1002/2017ja024406